

NJC

Accepted Manuscript



This is an *Accepted Manuscript*, which has been through the Royal Society of Chemistry peer review process and has been accepted for publication.

Accepted Manuscripts are published online shortly after acceptance, before technical editing, formatting and proof reading. Using this free service, authors can make their results available to the community, in citable form, before we publish the edited article. We will replace this *Accepted Manuscript* with the edited and formatted *Advance Article* as soon as it is available.

You can find more information about *Accepted Manuscripts* in the [Information for Authors](#).

Please note that technical editing may introduce minor changes to the text and/or graphics, which may alter content. The journal's standard [Terms & Conditions](#) and the [Ethical guidelines](#) still apply. In no event shall the Royal Society of Chemistry be held responsible for any errors or omissions in this *Accepted Manuscript* or any consequences arising from the use of any information it contains.

Table of contents

Bifunctional Pd/Fe₃O₄/charcoal nanocatalyst is synthesized by simple solid-state grinding. Highly loaded Pd and Fe₃O₄ nanoparticles are observed and exhibit high product time yield for Suzuki-Miyaura coupling reactions.



Facile Synthesis of Pd/Fe₃O₄/Charcoal Bifunctional Catalysts with High Metal Loading for High Product Yields in Suzuki- Miyaura Coupling Reactions

Hyunje Woo,^a Kyoungho Lee,^a Ji Chan Park^b and Kang Hyun Park*^a*

Department of Chemistry and Chemistry Institute for Functional Materials, Pusan National University, Busan 609-735, Korea, and Clean Fuel Laboratory, Korea Institute of Energy Research, Daejeon, 305-343, Korea.

E-mail: chemistry@pusan.ac.kr, jcpark@kier.re.kr

^a Pusan National University

^b Korea Institute of Energy Research

Abstract

In the present work, we synthesized magnetically separable Pd/Fe₃O₄/charcoal nanocatalysts by simple solid-state grinding of a mixture of salts and the simultaneous thermal decomposition of the salts. The highly loaded Pd nanoparticles (20 wt%) were well dispersed in the porous charcoal, with an average diameter of ~5 nm and clean surfaces without any surfactant. Moreover, the simultaneously obtained Fe₃O₄ nanoparticles (10 wt%) had good superparamagnetic character, enabling quick separation of the catalyst from the products and re-dispersion in the reaction solution. The bifunctional catalyst showed a high product time yield with various substituted aryl halides and aryl boronic acids.

Introduction

Pd-catalyzed C-C coupling reactions such as the Mizoroki-Heck and the Suzuki-Miyaura coupling reactions are of importance in many types of organic syntheses and in chemical, pharmaceutical, and agricultural industries.¹⁻⁵ Homogeneous palladium catalysts have been shown to exhibit high reaction rates and high turnover numbers (TONs). However, homogeneous catalysis has some critical drawbacks such as problems of reusing or recycling the catalyst, which lead to a significant loss of expensive metal. In industry, these problems pose a challenge that has yet to be overcome.

Until now, many studies have been focused on the catalytic activities of new types of supported Pd catalysts such as Pd@SiO₂ yolk-shell, Pd/graphene, and Pd/CMK-3, which showed high TOF (turnover frequency) values with very low Pd contents.⁶⁻⁹ In recent years, Kainz et. al. reported highly active Pd@Co/C nanocomposites with varying Pd loadings as an easily recyclable catalyst in alkene hydrogenation.¹⁰ However, commercially viable supported Pd catalysts for C-C coupling reactions are still required, which will ensure high product yields and the use of smaller amounts of the catalyst, as well as easy reuse. Practically, high metal loading with uniform particle dispersion in a supported catalyst can greatly enhance the product yield in catalytic reactions because there are more active sites in the same weight of catalyst, including the non-active support. It is possible to use a larger amount of the supported metal catalyst with a low metal content in the support, but this would significantly decrease the product yield per one reaction in an equally sized batch-type reactor. Finally, if the agglomeration is negligible, it is more advantageous to use a high-loaded metal catalyst for a compact reaction in a batch-type reactor than a higher amount of low-loaded metal catalyst.

To achieve a catalyst with high metal loading and high particle dispersion capacities, it is

necessary to use supports with high pore volume, such as mesoporous silica or carbon.^{9,11} High loading of metal precursors into a less porous support can cause severe agglomeration after thermal decomposition because the excessively impregnated metal salts are mainly located on the surface of the support. Carbon materials have shown high surface areas and large pore volumes, as well as good thermal and chemical stability.¹² Among the well-known activated carbons, activated charcoal obtained from wood could be the best candidate as a support, because of its large pore volume of $\sim 0.8 \text{ cm}^3 \cdot \text{g}^{-1}$ and large surface area, as well as its low cost.

For example, Pd on activated carbon (Pd/C) has been considered as a practical heterogeneous catalyst for C-C coupling reactions due its low cost, reusability, stability, simplicity, low level of residual Pd, and the absence of side reactions involving aryl-aryl exchanges.¹³⁻¹⁶ Chen et al. reported magnetically separable hybrid Pd/Fe₃O₄@charcoal catalysts, which are comprised of active 10 nm-sized Pd nanoparticles embedded in a 120 nm-sized iron oxide/carbon matrix.¹⁷ However, the synthesis of active metal nanoparticles with magnetic particles in the support still involves complex multi-step synthesis, which is especially difficult on a large scale. In industry, convenient catalyst preparation with a lower cost is an important issue, in addition to the activity and recyclability of the catalyst.

Recently, a solid-state grinding route consisting of grinding a mixed powder of the precursor and porous silica template, has been employed as an easy and fast method for the preparation of supported metal catalysts.^{11,18-20} The solid-grinding route (or melt-infiltration process) is well known as a solvent-free and convenient method of synthesizing supported catalysts. So far, to the best of our knowledge, there have been no reports of a bifunctional hybrid catalyst synthesized by a very simple solid-state grinding method of the mixed metal hydrate salts. Herein, we report the surfactant-free Pd/Fe₃O₄/charcoal bifunctional catalyst,

which consists of around 20 wt% of ~5 nm Pd and around 10 wt% of ~9 nm magnetite (Fe_3O_4) on activated charcoal.

Experimental Section

Chemicals. Palladium (II) nitrate dihydrate [$\text{Pd}(\text{NO}_3)_2 \cdot 2\text{H}_2\text{O}$] (~40% Pd basis), iron nitrate nonahydrate [$\text{Fe}(\text{NO}_3)_3 \cdot 9\text{H}_2\text{O}$] (ACS reagent, $\geq 98\%$) and activated charcoal (~100 mesh particle size, powder) were purchased from Aldrich. The chemicals were used as received without further purification.

Synthesis of the Pd/ Fe_3O_4 /charcoal catalyst. The commercial activated charcoal (DARCO) was used as obtained. To prepare the Pd(20wt%)/ Fe_3O_4 (10wt%)/charcoal catalyst, 0.36 g of $\text{Pd}(\text{NO}_3)_2 \cdot 2\text{H}_2\text{O}$ and 0.37 g of $\text{Fe}(\text{NO}_3)_3 \cdot 9\text{H}_2\text{O}$ were physically ground with 0.5 g of activated charcoal in a mortar for several minutes under ambient conditions until the color of the powder was homogeneously black. The mixed powder was then aged in a polypropylene bottle at 50 °C in an oven. After aging for 24 h, the sample was cooled under ambient atmosphere and transferred to an alumina boat in a tube-type furnace. Finally, the metal-incorporated charcoal powder was slowly heated at a ramping rate of 2.7 °C \cdot min⁻¹ up to 623 K under a nitrogen flow of 200 mL \cdot min⁻¹. The sample was held at 623 K for 4 h under a continuous nitrogen flow. For the preparation of the Pd(10wt%)/ Fe_3O_4 (10wt%)/charcoal catalyst, all procedures were identical to the synthesis of Pd(20wt%)/ Fe_3O_4 (10wt%)/charcoal, except for the use of 0.16 g of $\text{Pd}(\text{NO}_3)_2 \cdot 2\text{H}_2\text{O}$ and 0.33 g of $\text{Fe}(\text{NO}_3)_3 \cdot 9\text{H}_2\text{O}$.

Synthesis Pd(20wt%)/charcoal catalyst. To prepare the Pd(20wt%)/charcoal catalyst, 0.31 g of $\text{Pd}(\text{NO}_3)_2 \cdot 2\text{H}_2\text{O}$ were employed with 0.5 g of activated charcoal. The next procedures and conditions were identical to the synthesis of Pd(20wt%)/ Fe_3O_4 (10wt%)/charcoal.

General procedure for the Suzuki-Miyaura coupling reactions. The catalyst (generally 1.0

or 0.5 mol% with respect to the Pd content), 4-bromoanisole (0.12 mL, 1.0 mmol, 1.0 equiv), phenylboronic acid (0.14 g, 1.2 mmol, 1.2 equiv), potassium carbonate (0.26 g, 2.0 mmol, 2.0 equiv), DMF (10 mL), and water (2.5 mL) were mixed in a stainless steel reactor. The mixture was vigorously stirred at 100 °C. After the reaction, the reaction mixture was extracted with diethylether and potassium hydroxide solution to remove remaining boronic acid. Drying with MgSO₄, filtration, and solvent evaporation of the filtrate yielded the reaction products.

Recyclability and Pd leaching tests. After the reaction, the catalyst particles were separated by external magnet. The recovered particles were reused as a catalyst for the next reaction. For checking Pd leaching degree, poly(4-vinylpyridine) (PVPy) (300 equiv. with respect to the total Pd content) was employed prior to initiation of the reactions.

Characterization. The catalyst particles were characterized by transmission electron microscopy (TEM) (Omega EM912 operated at 120 kV, Korea Basic Science Institute, and a Tecnai G2 F30 operated at 300 kV, KAIST) and energy dispersive X-ray spectroscopy (EDX) (attached to the F30 Tecnai). The particle dispersion was drop-cast on carbon-coated Cu grids (Ted Pellar, Inc). The x-ray powder diffraction (XRD) patterns were recorded on a Rigaku D/MAX-RB (12 kW) diffractometer. The Pd and Fe contents of the samples were determined with an inductively coupled plasma-atomic emission spectrometer (ICP-AES) (POLY SCAN 60 E). The nitrogen sorption isotherms were measured at 77 K using a TriStar II 3020 surface area analyzer. Before the measurements, the samples were degassed in vacuum at 573 K for 4 h. The coupling reaction products were analyzed by ¹H nuclear magnetic resonance (NMR) spectroscopy using a Varian Mercury Plus (300 MHz). Chemical shift values were recorded as parts per million (ppm) relative to tetramethylsilane as an internal standard unless otherwise indicated, and coupling constants are given in Hz. The magnetization data were

collected using a superconducting quantum interference device (SQUID) (MPMS-7, Quantum design).

Results and Discussion

Synthesis of the Pd/Fe₃O₄/charcoal hybrid catalyst. Scheme 1 demonstrates the overall synthetic procedure for the Pd/Fe₃O₄/charcoal hybrid catalyst. The active Pd and magnetic Fe₃O₄ nanoparticles were successfully embedded in the porous charcoal support via two simple steps: a co-solid-grinding step and a thermal decomposition step. In the first step, the mixture of hydrate salts, which consists of Pd(NO₃)₂•2H₂O and Fe(NO₃)₃•9H₂O complexes, was concurrently melt-infiltrated into mesoporous charcoal by grinding at room temperature and subsequent aging at 50 °C for 24 h in an oven. In the second step, the melt-infiltrated salt was decomposed into tiny Pd and Fe₃O₄ nanoparticles by thermal decomposition at 400 °C under a nitrogen atmosphere.

TEM image shows the incorporated Pd and Fe₃O₄ nanoparticles in the porous charcoal support (Fig. 1a). However, distinguishing the two different types of particles was quite difficult in the low-resolution TEM images (Fig. S1 in the ESI†). High-resolution TEM (HRTEM) analysis revealed the distinct lattice fringe images of the Pd and Fe₃O₄ particles (Fig. 1b). The small Pd nanoparticles are single crystals with an average diameter of 5 nm, and the lattice distance was observed to be 0.225 nm, well matched with the (111) planes of Pd. On the other hand, slightly larger Fe₃O₄ particles are observed, around 9 nm, and their lattice distance was measured to be 0.253 nm of the (311) planes. The high-angle annular dark-field scanning transmission electron microscopy (HAADF-STEM) image shows regions of varying brightness; relatively dark (spot 1) and bright (spot 2) areas in many particles can be observed (Fig. 1c). EDX show spots 1 and 2 to be Fe-rich and Fe-poor, respectively, compared to the Pd content (Fig. 1d). This means that the dark spots in the HAADF-STEM image primarily originate from light Fe atoms, whereas the bright spots are caused by heavier Pd atoms. XRD data in Fig. 1e show a face-centered cubic (fcc) structure of Pd (JCPDS No.

46-1043). The average size of the Pd cores is estimated to be 5.1 nm from the broadness of the (111) peak by the Debye-Scherrer equation; this is in good agreement with that observed in the TEM images.

N₂ sorption experiments at 77 K for the bare charcoal and the Pd/Fe₃O₄/charcoal exhibited type IV adsorption-desorption hystereses with delayed capillary evaporation at a relative pressure of 0.5, and the Brunauer-Emmett-Teller (BET) surface areas of the bare charcoal and the Pd/Fe₃O₄/charcoal were calculated to be 1010.4 m²•g⁻¹ and 538.2 m²•g⁻¹, respectively (Fig. 2a). The total pore volume of the Pd/Fe₃O₄/charcoal hybrid catalyst was 0.37 cm³•g⁻¹, which was lower than that of the initial charcoal support (0.85 cm³•g⁻¹). These low values of BET surface area and pore volume of the Pd/Fe₃O₄/charcoal catalyst were mainly attributed to the high loading of Pd and Fe in the charcoal. The Pd loading of the Pd/Fe₃O₄/charcoal was measured to be 19.2 wt% by ICP-AES, which agrees well with the calculated 20 wt% Pd content based on the amount of Pd hydrate salt used in the experiment. The size of the small pores, obtained from the desorption branches in both the bare charcoal and the Pd/Fe₃O₄/charcoal was 3.8 nm (Fig. 2b).

Based on its superparamagnetic character, Fe₃O₄ (magnetite) has been applied for the preparation of magnetically recyclable heterogeneous catalysts with catalytically active metals such as Pd, Pt, Ir, etc. The magnetic properties of the Pd/Fe₃O₄/charcoal hybrid catalyst were recorded using a SQUID magnetometer with fields up to 4 T and hysteresis loops of the samples recorded at 5 K and 300 K (Fig. 3a). The magnetite particles showed typical ferromagnetism at 5 K, whereas superparamagnetism was observed at 300 K (Fig. S2 in the ESI†). The saturation magnetizations (M_s) of Fe₃O₄ at 300 K and 5 K were determined to be 39.9 emu•g⁻¹ and 60.0 emu•g⁻¹, respectively. For the M versus T data, zero field cooled (ZFC) and field cooled (FC) measurements for the Pd/Fe₃O₄/charcoal were conducted, and

the magnetization for a field strength of 500 Oe showed an obvious blocking temperature peak at 200.5 K (Fig. 3b).

Suzuki-Miyaura coupling reactions with 4-bromoanisole and phenylboronic acid. The immobilized Pd nanoparticles on charcoal were employed as a heterogeneous catalyst for Suzuki-Miyaura coupling reactions (Table 1). The reactions were carried out with 4-bromoanisole and phenylboronic acid in the presence of 2 equiv. potassium carbonate in an organic solvent and water mixture (4:1). The catalyst loading was either 0.5 or 1.0 mol% Pd with respect to the substrate. The product was quantitatively analyzed using the ^1H NMR. In entry 1, the reactions were conducted with a catalyst loading of 1.0 mol% Pd for 30 h in a mixture of toluene and water. The reaction with Pd(20wt%)/Fe₃O₄(10wt%)/charcoal exhibited 59% conversion. In order to determine the most suitable solvent system for the catalyst, a preliminary screening of solvents was performed. The results showed that N,N-dimethylformamide (DMF):H₂O (4:1) was a suitable solvent system for this reaction (turnover frequency = 25) (Table 1, entries 2–4 and 8). As expected, lowering the reaction temperature and time effectively decreased the conversion (Table 1, entries 5 and 6). To demonstrate catalytic activity of the Pd/Fe₃O₄/charcoal catalyst by different mol% of active Pd atoms (0.5 and 1.0 mol%), the conversion rates of 4-bromoanisole versus time were also checked (Fig. S3 in the ESI†). Furthermore, the product time yields [$\text{g}_{\text{product}} \cdot \text{g}_{\text{Pd}}^{-1} \cdot \text{h}^{-1}$] were calculated to confirm that our Pd(20wt%)/Fe₃O₄(10wt%)/charcoal catalyst showed a high product yield per reaction time (Table 1). The Pd(20wt%)/Fe₃O₄(10wt%)/charcoal catalyst showed higher values (46.0) than previously reported Pd/C catalysts (Table S1 in the ESI†).^{21,22} Moreover, the Pd(20wt%)/Fe₃O₄(10wt%)/charcoal catalyst exhibited superior catalytic activity to commercially available Pd/charcoal catalysts under the same conditions (Table 1, entries 8 and 10).

The low activity of the commercial catalyst was mainly attributed to its relatively large and irregular particle sizes compared to the synthesized one, observed by TEM images (Fig. S4 in the ESI†). The synthesized Pd(20wt%)/charcoal catalyst showed also relatively low conversion of 76% in the optimized condition, compared to ~99% of Pd(20wt%)/Fe₃O₄(10wt%)/charcoal catalyst (Table 1, entries 7 and 8). The TEM image of the Pd(20wt%)/charcoal catalyst shows some agglomerates of Pd particles (Fig. S5 in the ESI†). This is because the Pd hydrate salt without Fe hydrate salt was not fully infiltrated during the impregnation process into the porous charcoal. In order to confirm the catalytic property of the Fe₃O₄ nanoparticles, Fe₃O₄ nanoparticles on charcoal were only used without Pd nanoparticles; however, no product was obtained (Table 1, entry 9).

Recycling and Pd leaching tests. The Pd(20wt%)/Fe₃O₄(10wt%)/charcoal catalyst after the coupling reaction could be totally separated by an external magnet owing to the superparamagnetic property of Fe₃O₄ particles.²³ The Pd(20wt%)/Fe₃O₄(10wt%)/charcoal catalyst was recycled three times under the same reaction conditions and its initial high activity was still maintained without any loss during the recycling process (Table 1, entries 11-13). The resulting catalysts were monitored by TEM and XPS analysis. The TEM images of the catalysts after reactions showed no significant agglomeration both in the Pd and Fe₃O₄ nanoparticles (Fig. S6 in the ESI†). In the XPS data for The Pd(20wt%)/Fe₃O₄(10wt%)/charcoal catalysts before and after the reaction, the most intensive peak is observed at a binding energy around 335.4 eV (3d_{5/2}), indicating their metallic Pd characteristics. (Fig. S7 in the ESI†). For the Pd leaching test, the filtrated solution after the catalytic reaction was checked by ICP-AES analysis, but the Pd content in the solution was too small and negligible to confirm the Pd leaching degree, measured to be 0.48 ppm. And, the coupling reaction in the presence of PVPy, which behaves as a poison to trap

homogeneous Pd species through chelation in the solution phase, shows no obvious change in catalytic activity.²⁴ Therefore, we believe that the Pd/Fe₃O₄/charcoal catalysts in our catalytic system catalyze the coupling reactions in a heterogeneous manner.

Reactivity and productivity comparison among catalysts in the Suzuki-Miyaura coupling reaction.

When the total product time yields [$\text{g}_{\text{product}} \cdot \text{g}_{\text{total catalyst}}^{-1} \cdot \text{h}^{-1}$] were calculated, the Pd(20wt%)/Fe₃O₄(10wt%)/charcoal catalyst with 0.5 mol% Pd exhibited the highest value (11.0) among some catalysts (Fig. 4). Because the Pd content of the Pd(20wt%)/Fe₃O₄(10wt%)/charcoal is much higher compared to that in the conventional catalysts, our Pd(20wt%)/Fe₃O₄(10wt%)/charcoal catalyst exhibits higher total product time yields, making it more environmentally benign and applicable in industrial purposes. The Pd(20wt%)/Fe₃O₄(10wt%)/charcoal catalyst also showed the better total product time yield than Pd(10wt%)/Fe₃O₄(10wt%)/charcoal catalyst, even though the Pd nanoparticles in the Pd(10wt%)/Fe₃O₄(10wt%)/charcoal catalyst were small and uniform (Fig. S8a in the ESI†). The peaks in the XRD spectrum of the Pd(10wt%)/Fe₃O₄(10wt%)/charcoal were well-matched to Pd phase (JCPDS #46-1043) and Fe₃O₄ phase (JCPDS #19-0629), respectively (Fig. S8b in the ESI†).

The high activity of the Pd/Fe₃O₄/charcoal catalyst could be also originated from clean Pd surfaces. In our preparation method, which included the melt-infiltration of salts and subsequent reduction steps, surfactant addition was not required. Recently, in terms of the catalytic activity, the negative effects of residual surfactant on the surface of Pd nanoparticles, which were generally synthesized by a solvothermal reaction, have been reported; strongly bound surfactants such as trioctylphosphine and oleylamine on the particle surface can hinder the diffusion of the reactant over the Pd surfaces.

Substrate effects in the Suzuki-Miyaura coupling reactions

The substrate scope of the Pd/Fe₃O₄/charcoal-catalyzed Suzuki-Miyaura coupling reaction of aryl halides is summarized in Table 2. This reaction can be extended to a wide variety of substituted aryl halides and aryl boronic acids, and high product time yields were also observed for various substituted products. The Pd/Fe₃O₄/charcoal catalyst led to the complete conversion of substrates with C-Br, C-Cl, and C-OTf bonds (Table 2, entries 1–3). In addition, in our catalytic system, electron-withdrawing substituents such as F and CF₃ or electron-donating ones such as OMe and Me, as well as sterically hindered aryl halides, were readily coupled with arylboronic acids in good yields (Table 2, entries 4–7). Moreover, the reactions of various aryl bromides, including electron-deficient substrates such as those containing COMe and CHO functional groups, proceeded readily with high reactivity and selectivity (Table 2, entries 8–10).

Conclusion

We have fabricated magnetically separable Pd/Fe₃O₄/charcoal nanocatalysts by simple solid-state grinding of the mixed salts and the simultaneous thermal decomposition of the salts. Highly active Pd nanoparticles with a clean surface were densely and uniformly loaded into the porous charcoal support and were easily separated and reused by employing magnetic Fe₃O₄ nanoparticles in the same charcoal support. The bifunctional Pd/Fe₃O₄/charcoal catalyst showed a high product time yield for Suzuki-Miyaura coupling. By a series of experiments, we have confirmed that the Pd/Fe₃O₄/charcoal exhibited higher catalytic activity than the commercially available Pd/charcoal.

Acknowledgment. This research was supported by Basic Science Research Program through

the National Research Foundation of Korea(NRF) funded by the Ministry of Science, ICT & Future Planning (No.2013R1A1A1A05006634) and Research and Development Program of the Korea Institute of Energy Research(KIER) (B4-2432-03). K. H. P thank to the TJ Park Junior Faculty Fellowship and LG Yonam Foundation. The authors highly appreciate Mr. Seong Bum Yoo (Hanbat National University, Republic of Korea) for his technical support.

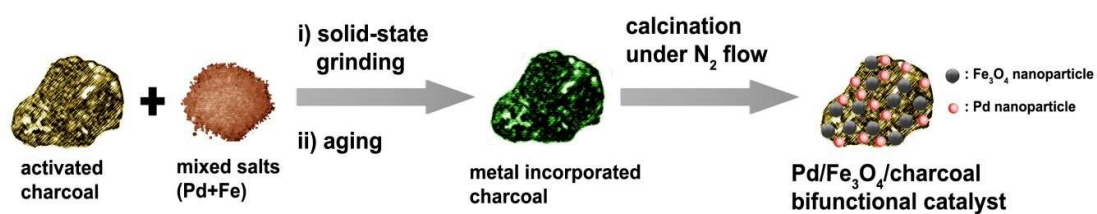
† Electronic supplementary information (ESI) available: the characterization of nanoparticle catalysts. See DOI:

References

1. I. P. Beletskaya and A. V. Cheprakov, *Chem. Rev.*, 2000, **100**, 3009.
2. N. Miyaura, and A. Suzuki, *Chem. Rev.*, 1995, **95**, 2457.
3. A. Balanta, C. Godard and C. Claver, *Chem. Soc. Rev.*, 2011, **40**, 4973.
4. N. Moitra, A. Matsushima, T. Kamei, K. Kanamori, Y. H. Ikuhara, X. Gao, K. Takeda, Y. Zhu, K. Nakanishi and T. Shimada, *New J. Chem.*, 2014, **38**, 1144
5. J. Niu, M. Liu, P. Wang, Y. Long, M. Xie, R. Li and J. Ma, *New J. Chem.*, 2014, **38**, 1471.
6. M. Kim, J. C. Park, A. Kim, K. H. Park, and H. Song, *Langmuir*, 2012, **28**, 6441.
7. S. Moussa, A. R. Siamaki, B. F. Gupton and M. S. El-Shall, *ACS Catal.*, 2012, **2**, 145.
8. H. R. Choi, H. Woo, S. Jang, J. Y. Cheon, C. Kim, J. Park, K. H. Park and S. H. Joo, *ChemCatChem*, 2012, **4**, 1587.

9. G. X. Pei, X. Y. Liu, A. Wang, L. Li, Y. Huang, T. Zhang, J. W. Lee, B. W. L. Jang and C-Y. Mou, *New J. Chem.*, 2014, **38**, 2043.
10. Q. M. Kainz, R. Linhardt, R. N. Grass, G. Vilé, J. Pérez-Ramírez, W. J. Stark and O. Reiser, *Adv. Funct. Mater.*, 2014, **24**, 2020.
11. T. M. Eggenhuisen, J. P. den Breejen, D. Verdoes, P. E. de Jongh and K. P. de Jong, *J. Am. Chem. Soc.*, 2010, **132**, 18318.
12. A. Schätz, T. R. Long, R. N. Grass, W. J. Stark, P. R. Hanson and O. Reiser, *Adv. Funct. Mater.*, 2010, **20**, 4323.
13. E. Guillén, R. Rico, J. M. López-Romero, J. Bedia, J. M. Rosas, J. Rodríguez-Mirasol and T. Cordero, *Appl. Catal. A*, 2009, **368**, 113.
14. L. Yin and J. Liebscher, *Chem. Rev.* 2007, **107**, 133.
15. S.-Y. Liu, H.-Y. Li, M.-M. Shi, H. Jiang, X.-L. Hu, W.-Q. Li, L. Fu and H.-Z. Chen, *Macromolecules*, 2012, **45**, 9004.
16. G. Lu, R. Franzén, Q. Zhanga and Y. Xu, *Tetrahedron Lett.*, 2005, **46**, 4255.
17. R. Li, P. Zhang, Y. Huang, P. Zhang, H. Zhong and Q. Chen, *J. Mater. Chem.*, 2012, **22**, 22750.
18. Y. M. Wang, Z. Y. Wu, L. Y. Shi and J. H. Zhu, *Adv. Mater.*, 2005, **17**, 323.
19. W. Yue, A. H. Hill, A. Harrison and W. Zhou, *Chem. Commun.*, 2007, **43**, 2518.
20. W. Yue and W. Zhou, *Chem. Mater.*, 2007, **19**, 2359.
21. C. R. LeBlond, A. T. Andrews, Y. Sun and J. R. Jr. Sowa, *Org. Lett.*, 2001, **3**, 1555.

22. A. Cassez, A. Ponchel, F. Hapiot and E. Monflier, *Org. Lett.*, 2006, **8**, 4823.
23. M. B. Gawande, P. S. Brancoa and R. S. Varma, *Chem. Soc. Rev.*, 2013, **42**, 3371.
24. J. C. Park, E. Heo, A. Kim, M. Kim, K. H. Park, and H. Song, *J. Phys. Chem. C*, 2011, **115**, 15772.



Scheme 1. The synthetic scheme of bifunctional Pd/Fe₃O₄/charcoal via co-solid-state grinding route.

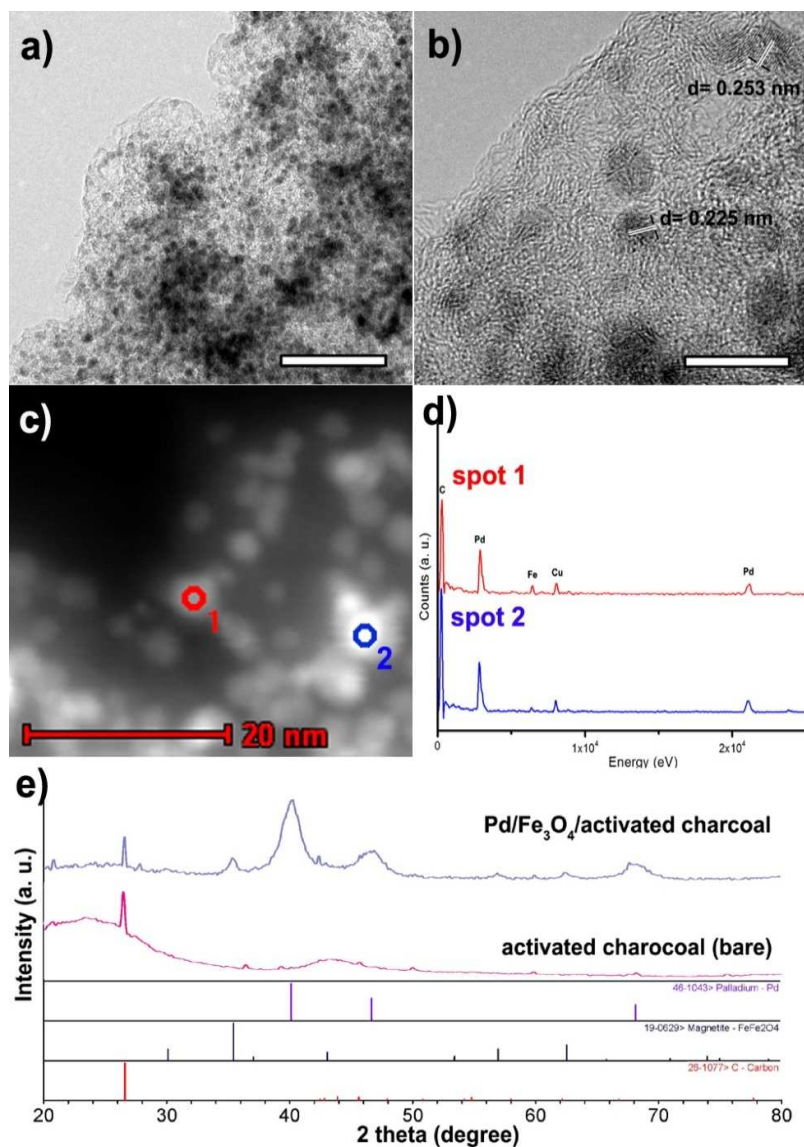


Fig. 1. (a) TEM, (b) HRTEM, and (c) HADDF-TEM images of Pd/Fe₃O₄/charcoal. (d) EDX spectra of (c). (e) XRD spectra of bare charcoal and Pd/Fe₃O₄/charcoal. The bars represent 50 nm (a) and 5 nm (b).

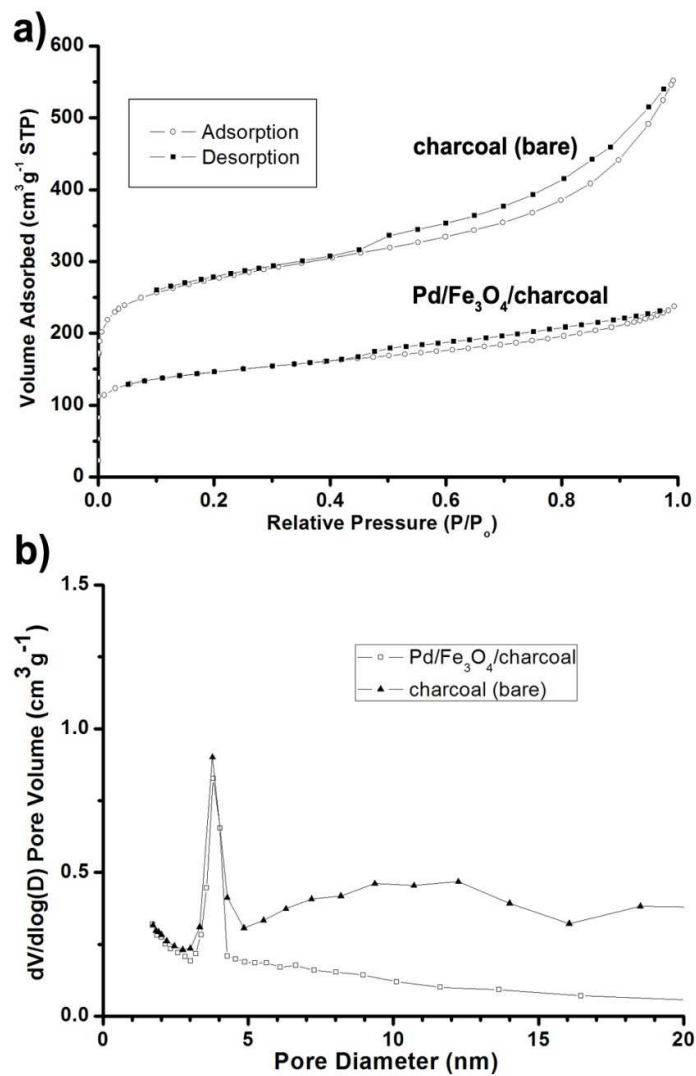


Fig. 2. (a) N_2 adsorption/desorption isotherms of bare charcoal and Pd/Fe₃O₄/charcoal, (b) pore size distribution diagrams calculated from desorption branches using the BJH method

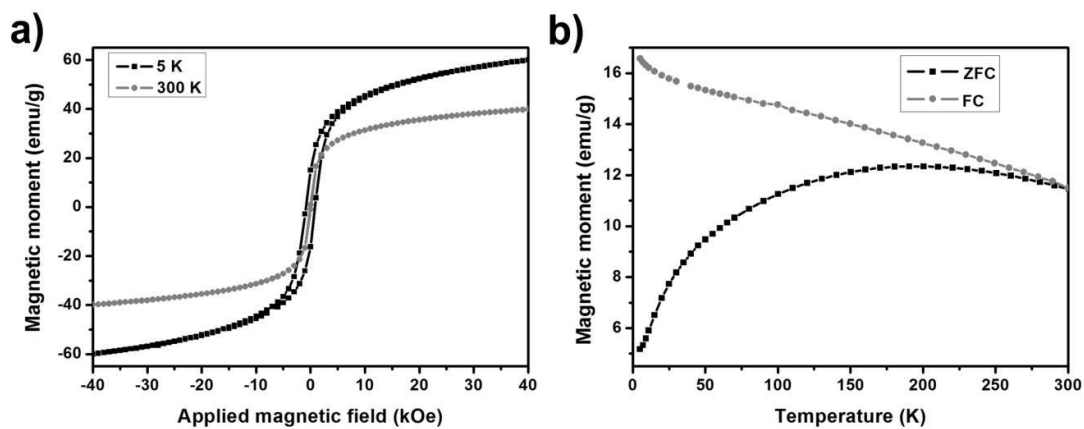
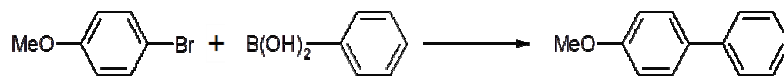


Fig. 3. (a) Magnetization-applied magnetic field (M-H) curve and ZFC/FC curve for Fe₃O₄ particles in Pd/Fe₃O₄/charcoal hybrid catalyst.

Table 1. Suzuki-Miyaura coupling reactions of 4-bromoanisole with phenylboronic acid

Entry	Catalyst	T [°C]	Time	Solvent	Conv. ^a [%]	Product time yield [g _{product} •g _{Pd} ⁻¹ •h ⁻¹]
1	Pd/Fe ₃ O ₄ /charcoal	150	30 h	Toluene/H ₂ O (4:1)	59	3.62
2	Pd/Fe ₃ O ₄ /charcoal	100	4 h	Toluene/H ₂ O (4:1)	4	1.84
3	Pd/Fe ₃ O ₄ /charcoal	100	4 h	DMSO/H ₂ O (4:1)	25	12.0
4	Pd/Fe ₃ O ₄ /charcoal	100	4 h	THF/H ₂ O (4:1)	35	15.1
5	Pd/Fe ₃ O ₄ /charcoal (Pd 0.5 mol%)	100	4 h	DMF/H ₂ O (4:1)	60	55.2
6	Pd/Fe ₃ O ₄ /charcoal	100	2 h	DMF/H ₂ O (4:1)	60	55.2
7	Pd/charcoal ^b	100	4 h	DMF/H ₂ O (4:1)	76	35.0
8	Pd/Fe ₃ O ₄ /charcoal	100	4 h	DMF/H ₂ O (4:1)	>99	46.0
9	Fe ₃ O ₄ /charcoal	100	4 h	DMF/H ₂ O (4:1)		No Rxn.
10	commercial Pd/charcoal	100	4 h	DMF/H ₂ O (4:1)	31	14.3
11	Recovered from #8	100	4 h	DMF/H ₂ O (4:1)	>99	46.0
12	Recovered from #11	100	4 h	DMF/H ₂ O (4:1)	>99	46.0
13	Recovered from #12	100	4 h	DMF/H ₂ O (4:1)	>99	46.0

Reaction conditions: Pd/Fe₃O₄/charcoal catalyst [5 mg (20 wt%), Pd base: 1.0 mol%], 4-bromoanisole (1.0 mmol), phenylboronic acid (1.2 mmol), K₂CO₃ (2.0 mmol), DMF (10.0 ml) and H₂O (2.5 ml). ^a Determined by using ¹H NMR spectroscopy based on 4-bromoanisole. ^b 20 wt% Pd NPs were used.

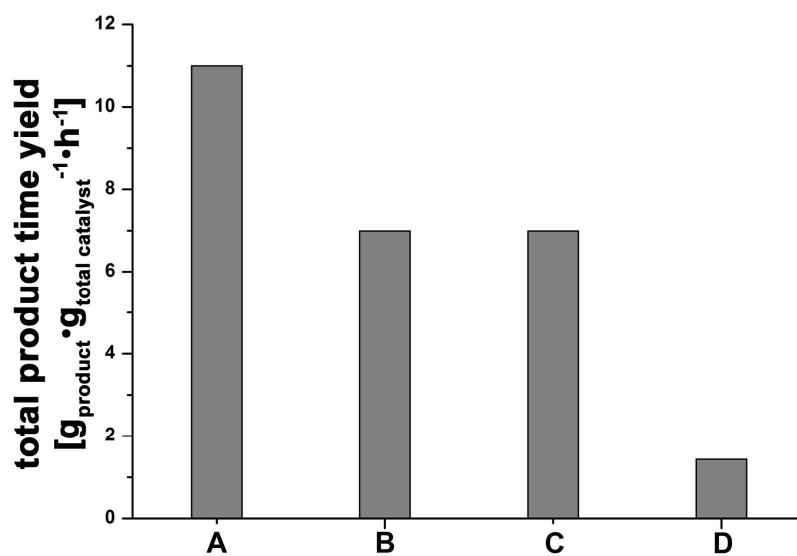
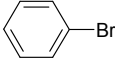
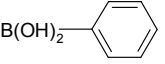
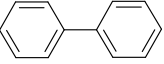
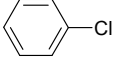
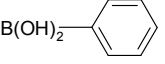
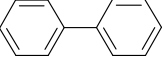
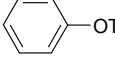
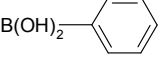
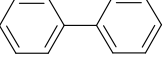
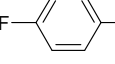
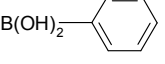
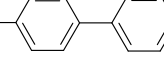
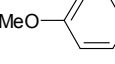
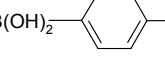
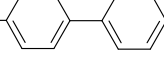
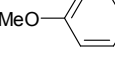
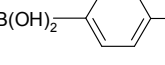
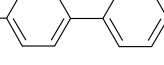
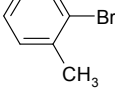
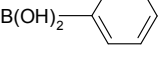
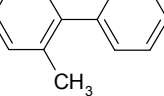
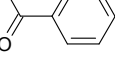
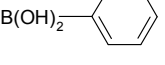
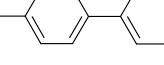
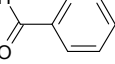
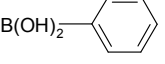
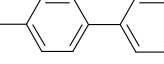
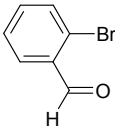
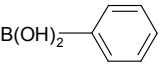
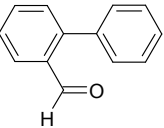


Fig. 4. Carbon coupling total product time yields for (A) Pd(20wt%)/Fe₃O₄(10wt%)/charcoal, (B) Pd(10wt%)/Fe₃O₄(10wt%)/charcoal, (C) Pd(20wt%)/charcoal and, (D) commercial Pd/charcoal. Each value per active Pd weight was calculated by reaction results in table 1 (total catalyst=Pd+Fe₃O₄+charcoal).

Table 2. Suzuki-Miyaura coupling reactions of arylhalides with arylboronic acid

Entry	Aryl halide	Boronic acid	Product	Yield ^a (%)	Product time yield [g _{product} •g _{Pd} ⁻¹ •h ⁻¹]
1				> 99	36.2
2				> 99	36.2
3				> 99	36.2
4				> 99	43.1
5				45	20.9
6				64	37.9
7				48	18.9
8				99	48.6
9				83	35.5
10				90	38.5

Reaction conditions: arylhalide (1.0 mmol), boronic acid (1.2 mmol), K₂CO₃ (2.0 mmol), DMF (10.0 ml), H₂O (2.5 ml), Pd/Fe₃O₄/charcoal catalyst (1.0 mol%), 100 °C, 4 h. ^a Determined by using GC-MS Spectroscopy based on arylhalides.